Cascade calculation of K^--p and K^--d atoms

T. Koike
Department of Physics, Hokkaido University, Sapporo 060, Japan

T. Harada
Department of Social Information, Sapporo Gakuin University, Ebetsu 069, Japan

Y. Akaishi
Institute for Nuclear Study, University of Tokyo, Tanashi, Tokyo 188, Japan
(Received 15 September 1995)

X-ray yields of K^--p and K^--d atoms are calculated as a function of the target density in order to find an optimum condition for experiments. The dependence of the yields on the energy level shift and absorption width due to the strong interaction is systematically investigated.

PACS number(s): 25.80.Nv, 13.75.Jz, 36.10.Gv

I. INTRODUCTION

The KN interaction at low energy is an important subject to be studied as the strong interaction with strangeness, especially concerning the $\Lambda(1405)$ puzzle [1]. The problem, however, is in a confusing situation at present. Previous x-ray measurements of K^--p atoms [2–4] are quite unsatisfactory due to their poor statistics. Moreover, all the experiments suggested an ''attractive'' interaction, while theories predicted a ''repulsive'' interaction [5–11]. Here, ''attractive'' and ''repulsive'' mean downward and upward shifts of the atomic 1s level, respectively.

In order to resolve this problem from the experimental side, a precise measurement of K^--p atom x rays is now going on at KEK [12]. A measurement of K^--d may also be done in the future. In the K^--p experiment, a gas hydrogen target is used, since the x-ray yield is reduced due to Stark mixing in the case of a liquid hydrogen target used in the previous experiments. In the case of a gas target, however, the K^- stopping efficiency is low because of the short lifetime of K^-. In addition, the weak decay of K^- occurs during the atomic cascade process in the case of a dilute gas target. Therefore, the density dependence of the x-ray yield should be investigated in order to find an optimum condition of the target for the experiment.

Although atomic cascade calculations of the K^--p atom were already carried out by several authors [13–15], their results did not agree with each other since different absorption widths were used. Therefore, a systematic study should be organized of the dependence of the cascade process on strong-interaction parameters. The purpose of this paper is to calculate the K^--p and K^--d atom x-ray yields as a function of target density for a guide to planning the experiment. The dependence of the yield on the energy shift and the absorption width is also systematically investigated in order to get the strong-interaction parameters from experimental x-ray yields.

The outline of this paper is as follows: In Sec. II, the method of cascade calculation is summarized and is applied to $\bar{p}$-p and $\bar{p}$-d atoms to determine the parameters in our cascade model. The results of K^--p atoms are given in Sec. III and those of K^--d atoms in Sec. IV. Finally, conclusions are given in Sec. V.

II. METHOD OF CASCADE CALCULATION

A. Cascade model

So far, there are two types of cascade models for the exotic hydrogen atom. The most elaborate cascade model would be Mainz's Monte Carlo simulation [15,16], which has no free parameter, but this model involves too much computation to investigate systematically the dependence of x-ray yields on many sets of strong-interaction parameters. We employ the other one, the standard Borie-Leon model, which was used in Refs. [13,14]. Though this model includes free parameters, it can reproduce the known x-ray yields when relevant parameters are adjusted. Since the Borie-Leon model is described in detail in Refs. [13,17], we present only a list of the processes and their transition rates included in the cascade calculation.

In this subsection, X^- denotes a heavy negatively charged particle and all transition rates are given in atomic units ($m_e = e = \hbar = 1$).

(1) Molecular dissociation $(X^- p)_i + H_2 \rightarrow (X^- p)_f + H + H$: If the transition energy $\Delta E_{if} \equiv E_i - E_f \geqslant 4.7$ eV (dissociation energy of H_2 molecules),

$$\Gamma^{\mathrm{mol}}_{n,l\rightarrow n',l} = \frac{N}{2} v \pi a_n^2, \tag{1}$$

where N is the target density of hydrogen atoms ($\approx 4.25\times 10^{22}$ cm^{-3} at liquid hydrogen), v the velocity of the exotic atom, and a_n the nth Bohr orbit of the exotic atom. In our model, only the Δn = minimum case is taken and $\Delta l = 0$ is assumed.[1]

[1]In Ref. [13], there was no statement concerning the n' and l' dependence, but the original program code written by Borie and Leon included such a dependence. Note that the l' dependence has little influence on the final results, but the n' dependence affects significantly the x-ray yield for high density targets.

(2) External Auger transition $(X^-p)_i + \mathrm{H} \rightarrow (X^-p)_f + \mathrm{H}^+ + e^-$: If $\Delta E_{if} \geqslant 15.6$ eV (ionization energy of H_2 molecules),

$$\Gamma^{\mathrm{Aug}}_{n,l\rightarrow n',l'} = \frac{16}{3}\pi\frac{N}{\mu^2}(R^{n,l}_{n',l'})^2\frac{\mathrm{Max}(l,l')}{2l+1}(2\Delta E+1.39)^{-1/2}, \tag{2}$$

where μ is the reduced mass of the exotic atom, $\Delta E = \Delta E_{if} - 15.6$ eV,[2] and $R^{n,l}_{n',l'}$ is the radial matrix element for the transition from n,l to n',l' with $l' = l \pm 1$.

(3) Radiative transition $(X^-p)_i \rightarrow (X^-p)_f + \gamma$:

$$\Gamma^{\mathrm{rad}}_{n,l\rightarrow n',l'} = \frac{4}{3}\alpha\mu^{-2}(R^{n,l}_{n',l'})^2\frac{\mathrm{Max}(l,l')}{2l+1}(\Delta E_{if})^3, \tag{3}$$

where α is the fine structure constant.

(4) Nuclear absorption:

$$\Gamma^{\mathrm{abs}}_{ns} = \Gamma^{\mathrm{abs}}_{1s}/n^3, \tag{4}$$

$$\Gamma^{\mathrm{abs}}_{np} = \frac{32}{3}\frac{n^2-1}{n^5}\Gamma^{\mathrm{abs}}_{2p}, \tag{5}$$

$$\Gamma^{\mathrm{abs}}_{nd} = \frac{2187}{40}\frac{(n^2-1)(n^2-4)}{n^7}\Gamma^{\mathrm{abs}}_{3d}. \tag{6}$$

$\Gamma^{\mathrm{abs}}_{1s}$, $\Gamma^{\mathrm{abs}}_{2p}$, and $\Gamma^{\mathrm{abs}}_{3d}$ are taken from experimental values or calculated values with a relevant optical potential. Otherwise, they are treated as parameters.

(5) Stark mixing $(X^-p)_i + \mathrm{H} \rightarrow (X^-p)_f + \mathrm{H}$: For $l>1$, [3]

$$\Gamma^{\mathrm{Stark}}_{n,l\rightarrow n,l+1} = \frac{2l+1}{2l-1}\Gamma^{\mathrm{Stark}}_{n,l\rightarrow n,l-1} = k_{\mathrm{stk}} N v \pi\rho_0^2 \tag{7}$$

where k_{stk} is a free parameter and the effective impact parameter ρ_0 is the root of the equation

$$\frac{v\mu}{2n^2} = \frac{1}{\pi\rho}\int_{-\pi/2}^{\pi/2} e^{-2\rho\ \sec\theta}(1+2\rho\ \sec\theta+2\rho^2\sec^2\theta)d\theta. \tag{8}$$

For the mixing between s and p orbits,[4]

$$\Gamma^{\mathrm{Stark}}_{n,s\rightarrow n,p} = 3\Gamma^{\mathrm{Stark}}_{n,p\rightarrow n,s} = k_{\mathrm{stk}} N v \pi\rho_0'^2, \tag{9}$$

where ρ_0' $(<\rho_0)$ is taken as $\rho_0' = \mathrm{Max}(R_0,\rho_1)$, R_0 is the root of the equation

$$\frac{\mu|\delta E_{ns}|_{\mathrm{eff}}}{3n^2} = 0.58\left(1+\frac{1}{R}+\frac{1}{2R^2}\right)\exp(-2R), \tag{10}$$

and ρ_1 is the root of

$$\frac{v\mu^2|\delta E_{ns}|^2_{\mathrm{eff}}}{3n^3\Gamma^{\mathrm{abs}}_{ns}} = \frac{1}{\rho^3}\int_{-\pi/2}^{\pi/2} e^{-4\rho\ \sec\theta} \times(1+2\rho\ \sec\theta+2\rho^2\sec^2\theta)^2\ \sec^{-2}\theta\, d\theta. \tag{11}$$

The effective energy shift $|\delta E_{ns}|_{\mathrm{eff}}$ is the magnitude of complex energy shift, given by

$$|\delta E_{1s}|_{\mathrm{eff}} = \left|(\delta E_{1s})_{\mathrm{strong}} + (\delta E_{1s})_{\mathrm{VP}} + (\delta E_{1s})_{\mathrm{FS}} - i\frac{\Gamma^{\mathrm{abs}}_{1s}}{2}\right|, \tag{12}$$

$$|\delta E_{ns}|_{\mathrm{eff}} = |\delta E_{1s}|_{\mathrm{eff}}/n^3. \tag{13}$$

Here, since the real part of δE_{1s} is not the shift from the QED value but from the nonrelativistic point-Coulomb energy, it contains the shift due to vacuum polarization, $(\delta E_{1s})_{\mathrm{VP}}$, and finite size effects, $(\delta E_{1s})_{\mathrm{FS}}$, besides the shift due to the strong interaction, $(\delta E_{1s})_{\mathrm{strong}}$. (It is assumed that other corrections for the $1s$ state and the shift of np states are negligible.)

(6) Weak decay Γ^{weak}: It is important for a dilute gas target to take into account the weak decay of X^- (except for antiprotons).

The initial distribution of X^- is taken to be proportional to $(2l+1)$ at $n \sim \sqrt{\mu/m_e}$, where the orbit size corresponds to the electron $1s$ Bohr radius. The shape of the angular momentum distribution does not affect the final results, since Stark mixing shuffles the population among states with the same n but different l, and its initial distribution is forgotten even for about 0.1 atom gas target.

B. Application to antiprotonic and pionic atoms

In order to check our cascade model[5] and to determine the value of the free parameter k_{stk} in Eqs. (7) and (9), a fitting to the known x-ray yields is done. In Ref. [13], k_{stk} was taken to range from 1 to 5, since there were poor experimental data at that time. Now, there exist numerous x-ray data for the $\bar{p}$-p and $\bar{p}$-d atoms at various target densities [18,19]. Recently, the density dependences of π^--p and π^--d atom x-ray data were obtained [20]. These data enable us to put more restrictions on k_{stk}. The results for the fitting to these data are shown in Figs. 1–4. The x-ray yields are well reproduced when $k_{\mathrm{stk}} = 2.0 \pm 0.5$ and the kinetic energy $T = 1$ eV. As for

[2] In Ref. [13], Eq. (2) was written as if ΔE was confused with ΔE_{if}. The original code, however, is written using the correct formula.

[3] Equation (7) was given incorrectly in Ref. [13], but the original program used the correct equation. This was already pointed out by Batty in Ref. [18].

[4] Equation (9) was also given incorrectly in Ref. [13], but the original program used the correct equation.

[5] We could not exactly reproduce the results in Ref. [13] in spite of the fact that same parameters were used. We ascertained that our code and the original Borie-Leon code, which were written independently, gave the same results when the same parameters were used. Therefore, we believe that our results are correct. The disagreement, however, is not so serious because the difference between our results and those in Ref. [13] is located within the uncertainty of k_{stk}.

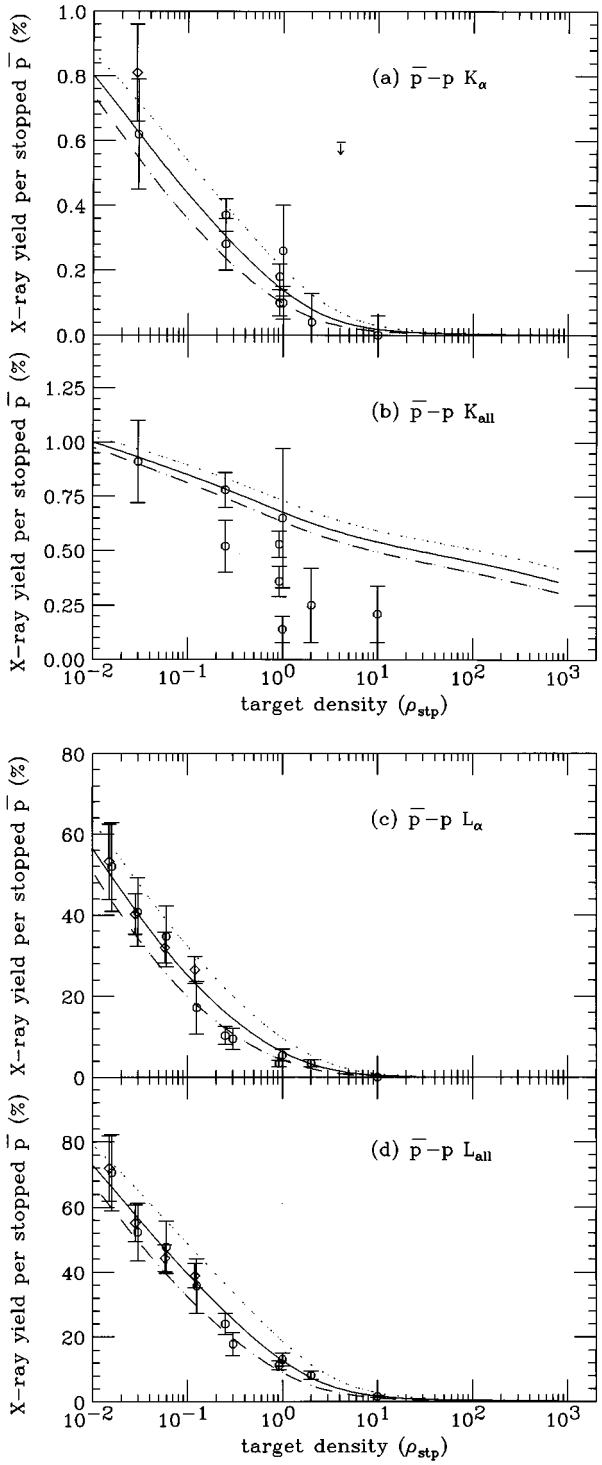

FIG. 1. Density dependence of $\bar{p}$-p atom x-ray yields. (a) K_α, (b) $K_{\rm all}$, (c) L_α, (d) $L_{\rm all}$. The unit of the horizontal line is $\rho_{\rm stp}$, the hydrogen atom density at a standard temperature (273 K) and pressure (one atom). The dotted line denotes $k_{\rm stk} = 1.5$, the solid line $k_{\rm stk} = 2.0$, and the dashed line $k_{\rm stk} = 2.5$. The strong-interaction parameters are $(\delta E_{1s})_{\rm strong} = -0.730$ keV (repulsive), $\Gamma_{1s}^{\rm abs} = 1.122$ keV, and $\Gamma_{2p}^{\rm abs} = 34$ meV [19]. $(\delta E_{1s})_{\rm VP} = 42$ eV and $(\delta E_{1s})_{\rm FS} = -3$ eV are also taken into account for $|\delta E_{1s}|_{\rm eff}$ [18]. The experimental data taken before 1989 (circles) are listed in Ref. [18] and new data [20] (diamonds) are added.

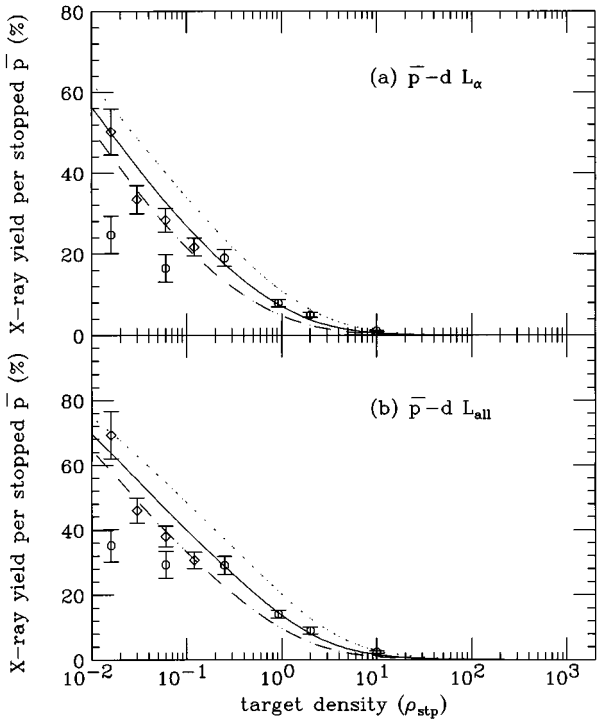

FIG. 2. Density dependence of $\bar{p}$-d atom x-ray yields. (a) L_α, (b) $L_{\rm all}$. The strong-interaction parameters are $(\delta E_{1s})_{\rm strong} = -2.14$ keV, $\Gamma_{1s}^{\rm abs} = 1.26$ keV, $\Gamma_{2p}^{\rm abs} = 0.4$ meV, and $\Gamma_{3d}^{\rm abs} = 5$ μeV [18]. $(\delta E_{1s})_{\rm VP} = 67$ eV and $(\delta E_{1s})_{\rm FS} = -48$ eV are also taken into account for $|\delta E_{1s}|_{\rm eff}$ [18]. Other details are same as in Fig. 1. The calculation well reproduces the new data (diamonds) at low densities.

the $\bar{p}$-p atom and $\bar{p}$-d atom, these results are consistent with other calculations reviewed by Batty [18] using the standard Borie-Leon model.

Of course, the use of the adjustable parameter $k_{\rm stk}$ and T is phenomenological. From a more realistic viewpoint, x-ray data should be reproduced by not using $k_{\rm stk}$ and including the distribution of kinetic energy. Mainz's model has no parameter concerning the Stark-mixing process; however, it does not consider the acceleration of exotic hydrogen atoms [16]. The measurement of the π^--p atom kinetic energy distribution showed a high energy component ranging from 1 eV to 70 eV besides a distribution around 1 eV [21]. For this reason, the authors of Ref. [20] extended the Borie-Leon approach by including the kinetic energy distribution; however, $k_{\rm stk} \sim 1.5$ was still needed in order to fit the measured π^--p atom x-ray yields. Although a refinement of the cascade model would be necessary in the future, the standard Borie-Leon model can reproduce x-ray yields of π^--p and π^-d atoms with $k_{\rm stk} = 2.0 \pm 0.5$ and $T = 1$ eV. If T is somewhat varied, almost the same results can be obtained by changing $k_{\rm stk}$ to some degree. From these results, we also use $k_{\rm stk} = 2.0$ and $T = 1$ eV for the K^--p and K^--d atoms and the uncertainty of $k_{\rm stk}$ is considered to be ± 0.5.

III. RESULTS OF KAONIC HYDROGEN

In the case of K^--p atoms, three experiments for liquid targets were reported [2–4]. The experimental results and

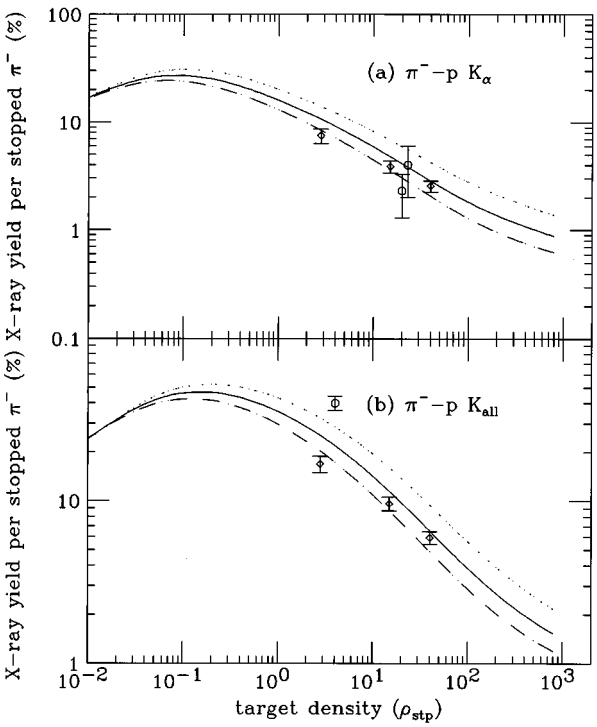

FIG. 3. Density dependence of π^--p atom x-ray yields. (a) K_α, (b) $K_{\rm all}$. The strong-interaction parameters are $(\delta E_{1s})_{\rm strong}$ = 7.1 eV (attractive), $\Gamma_{1s}^{\rm abs}$ = 0.8 eV. $(\delta E_{1s})_{\rm VP}$ = 3.2 eV are also taken into account for $|\delta E_{1s}|_{\rm eff}$. Experimental data are taken from Ref. [25].

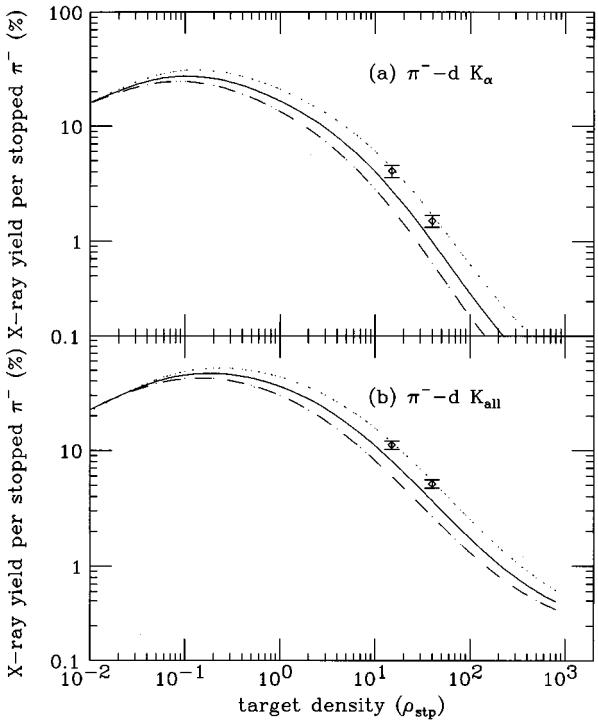

FIG. 4. Density dependence of π^--d atom x-ray yields. (a) K_α, (b) $K_{\rm all}$. The strong-interaction parameters are $(\delta E_{1s})_{\rm strong}$ = −2.5 eV (repulsive), $\Gamma_{1s}^{\rm abs}$ = 1.0 eV. $(\delta E_{1s})_{\rm VP}$ = 3.7 eV and $(\delta E_{1s})_{\rm FS}$ = −0.5 eV are also taken into account for $|\delta E_{1s}|_{\rm eff}$. Experimental data are taken from Ref. [26].

theoretical predictions of the energy shift and width are listed in Table I. Here, the sign of the energy shift is defined as the positive value is attractive. By the formula of Deser *et al.*, [22] the scattering length a is related to the energy shift and width as

$$2\mu^2\alpha^3 a=(\Delta E_{1s})_{\rm strong}+i\frac{\Gamma_{1s}^{\rm abs}}{2}. \tag{14}$$

The vacuum polarization $(\delta E_{1s})_{\rm VP}$ is about 25 eV [13]. As shown in Table I, the sign of the energy shift is opposite between the theories and the experiments. However, the Stark mixing depends on the magnitude of the effective energy shift $|\delta E_{1s}|_{\rm eff}$ without regard to its sign. Thus, the sign is not important for the cascade process. Although radiative transition rates would be changed from QED values, we assume that the use of accurate transition rates brings no significant improvement, considering the uncertainty in the treatment of other processes, and for simplicity we use nonrelativistic and point-Coulomb matrix elements.

Figure 5 shows the dependence of x-ray yields on the $1s$ energy shift $(\delta E_{1s})_{\rm strong}$ and the absorption width $\Gamma_{1s}^{\rm abs}$ with fixing $\Gamma_{2p}^{\rm abs}$. We show only results for the parameter sets of Tanaka and Suzuki [11] and of Conboy *et al.* [10] in Table I, which suffer the weakest and strongest Stark effects, respectively. The other cases in Table I lie between these two cases. The decrease of x-ray yields for higher density is due to the high-ns absorption resulting from the strong Stark mixing. Note that the larger $\Gamma_{1s}^{\rm abs}$ does not always reduce the x-ray yields at high density compared to the smaller $\Gamma_{1s}^{\rm abs}$, since the absorption rate through the Stark-mixed s state depends on not only $\Gamma_{1s}^{\rm abs}$ but also on $|\delta E_{1s}|_{\rm eff}$. It roughly depends on $\Gamma_{1s}^{\rm abs}/|\delta E_{1s}|_{\rm eff}^2$ as seen from Eq. (11). The uncertainty shown in Fig. 5 is nearly same as that corresponding to the range over $k_{\rm stk}$=1.5–2.5, as shown in Fig. 7 below.

The decrease of x-ray yields for lower density, which was not observed in the case of $\bar{p}$-p atoms, comes from the weak decay of K^- on an atomic orbit due to the long cascade time. A similar situation is expected in the case of pionic atoms as shown in Figs. 3 and 4. The weak decay was not included in Ref. [15], where the x-ray yields monotonically increase as the target density decreases. The weak decay rate is independent of strong interactions but has a slight dependence on the initial distribution.

Figure 6 shows the dependence of the x-ray yields on the $2p$ absorption width $\Gamma_{2p}^{\rm abs}$ when $\Gamma_{1s}^{\rm abs}$ and $(\delta E_{1s})_{\rm strong}$ are fixed. As shown in the figures, $\Gamma_{2p}^{\rm abs}$ is an important factor for the prediction of the absolute yield. There is a tendency for the K_α yield to become maximum at about one atom, K_β to be almost constant between one atom and liquid ($790\rho_{\rm stp}$) and K_γ to become maximum at high density near liquid. If we consider the old experimental x-ray yields [2–4] as upper limits, $\Gamma_{2p}^{\rm abs}>$ 1 meV is needed by comparing the calculated K_α and K_β yields with the experimental ones, while the calculated K_γ yields are larger than the experimental ones even the case that $\Gamma_{2p}^{\rm abs}$= 5 meV. The direct measurement of $\Gamma_{2p}^{\rm abs}$ is impossible since it is much smaller than the detector resolution. Alternatively, the L lines are available for determining $\Gamma_{2p}^{\rm abs}$. The ratio of $K_\alpha/L_{\rm all}$ for a gas target makes it possible to determine the $2p$ width by the relation [18]

TABLE I. Theoretical predictions of the energy shift and width of K^--p atoms and experimental data obtained by the previous x-ray measurements. The energy shift, defined as positive, is attractive.

	Scattering length a (fm)	$(\delta E_{1s})_{\rm strong}$ (eV)	$\Gamma_{1s}^{\rm abs}$ (eV)	Refs.
Theories				
Kim	-0.76 + i0.72	-313	594	[5]
Chao *et al.*	-0.87 + i0.70	-358	577	[6]
Martin and Ross	-0.90 + i0.67	-371	552	[7]
Martin	-0.66 + i0.64	-272	528	[8]
Dalitz *et al.*	-0.73 + i0.63	-301	519	[9]
Conboy *et al.*	-0.09 + i0.84	-37	692	[10]
Tanaka and Suzuki	-1.11 + i0.70	-457	577	[11]
Experiments				
Davis *et al.*	$+0.11\pm0.14 + i0.00^{+0.28}_{-0.00}$	$+45\pm58$	0^{+230}_{-0}	[2]
Izycki *et al.*	$+0.65\pm0.19 + i0.68\pm0.31$	$+268\pm78$	561 ± 256	[3]
Bird *et al.*	$+0.47\pm0.14 + i0.31^{+0.27}_{-0.10}$	$+194\pm58$	82^{+220}_{-82}	[4]

$$\frac{K_\alpha \text{ yield}}{L_{\rm all} \text{ yield}} = \frac{\Gamma^{\rm rad}_{2p\to 1s}}{\Gamma^{\rm rad}_{2p\to 1s}+\Gamma^{\rm abs}_{2p}}. \tag{15}$$

Figure 7 shows uncertainties coming from the not-well-determined parameter $k_{\rm stk}$. The hatched areas correspond to the range of the Stark parameter $k_{\rm stk}=1.5-2.5$. It should be noted that for a liquid target, K_β and K_γ are stronger than K_α due to the large Stark mixing rate even when the theoretical errors are taken into account. Reference [4] reported an anomalously large K_β/K_α ratio together with a small K_γ/K_α ratio. The old experimental data should be reexamined by considering the large K_β and K_γ yields.

In Fig. 8, we demonstrate a stream of the cascade-down process. The populations at very high-n states distribute with nearly statistical $(2l+1)$ weight. This is due to the large Stark-mixing rate, not because the initial distribution is taken to be statistical. In the case of a liquid target, the absorption occurs from s orbits, mainly $3s-6s$. On the other hand, in the case of a gas target the p-orbit absorption increases, because the Stark effect in the low-n region is weaker than that in the case of a liquid. However, the fact that the population for the high-n region seems similar to those of a liquid means that the Stark effect still dominates in high-n states even for a gas target.

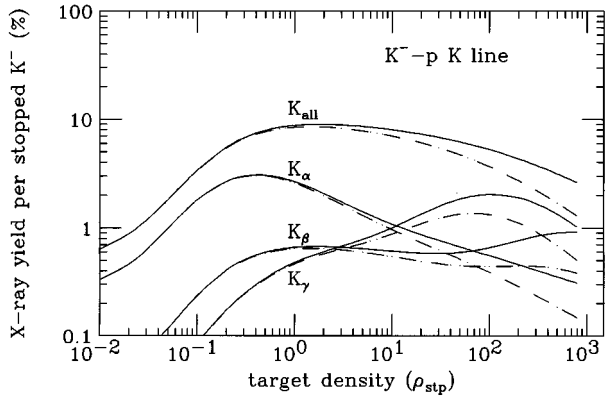

FIG. 5. Density dependence of K^--p atom x-ray yields with varying $(\delta E_{1s})_{\rm strong}$ and $\Gamma_{1s}^{\rm abs}$. The solid lines and the dashed lines are the cases which suffer the strongest (Conboy *et al.* [10]) and the weakest (Tanaka and Suzuki [11]) Stark effects among the parameters given in Table I, respectively. The other cases in Table I lie between these lines. The width $\Gamma_{2p}^{\rm abs}$ is taken to be 1 meV. The free parameter $k_{\rm stk}$ is fixed to 2.0.

Finally, we show the expected x-ray spectrum at various target densities. In Fig. 9, the peak distribution is assumed to be of Lorentzian form without including the detector resolution. As is shown in the figures, $K_{\geqslant\beta}$ lines form a superposed peak around 8 keV. In order to make a direct measurement of $(\delta E_{1s})_{\rm strong}$ and $\Gamma_{1s}^{\rm abs}$, the K_α line ($\sim$6.5 keV) must be well separated from the $K_{\geqslant\beta}$ lines. It would be also possible to extract the shift and width from the superposed $K_{\geqslant\beta}$ lines with the help of the cascade calculation, though its accuracy would be lower than those from the direct measurement of the K_α yield. The ratio $K_\alpha/K_{\geqslant\beta}$ becomes larger as the target density becomes lower. Thus, the liquid target is not suitable for a precise determination of the shift and width, in spite of a large stopping power of K^-.

At a seven-atom gas target, which corresponds to the experiment at KEK [12], the K_α peak would be barely recognized when the detector resolution is considered. Of course, the smaller $\Gamma_{2p}^{\rm abs}$ makes the K_α yield larger. However, $\Gamma_{2p}^{\rm abs} > 1$ meV is suggested from the old experiments, as discussed in Fig. 6. The ratio $K_\alpha/K_{\geqslant\beta}$ as well as the ratio $K_\alpha/L_{\rm all}$ gives information about the width $\Gamma_{2p}^{\rm abs}$. To guarantee a clear observation of K_α, a lower density target is favorable even though it sacrifices the stopping efficiency of K^-. A gas target of about one atom would be the most appropriate case, since the absolute K_α yield becomes maximum at this density.

IV. RESULTS OF KAONIC DEUTERIUM

Since there exist no x-ray data for K^--d atoms, the energy shift and the absorption width are obtained by solving a Klein-Gordon equation with a relevant optical potential. The equation is

$$\left[\left(1+\frac{\omega}{M_A}\right)\nabla^2+(\omega-V_{\rm Coul})^2-\mu^2\right]\chi = 2\omega V_{\rm strong}\chi, \tag{16}$$

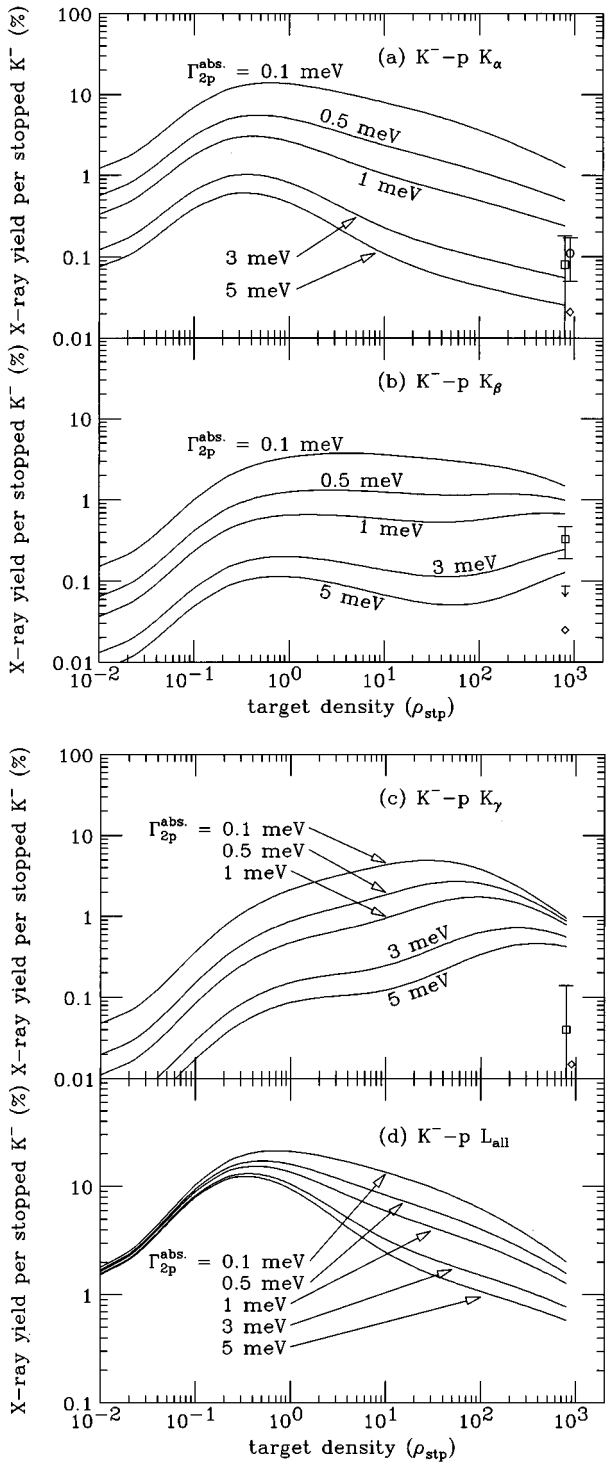

FIG. 6. Density dependence of K^--p atom x-ray yields with varying $\Gamma_{2p}^{\rm abs}$. (a) K_α, (b) K_β, (c) K_γ, (d) L_α. The shift and width are taken to be $|\delta E_{1s}|_{\rm eff}$ = 300 eV and $\Gamma_{1s}^{\rm abs}$ = 550 eV, which are nearly averages of the theoretical values. The free parameter $k_{\rm stk}$ is fixed to 2.0. Experimental data are taken from Refs. [2–4].

with

$$2\omega V_{\rm strong} = -4\pi\left(1+\frac{\omega}{M}\right)\bar{a}\rho(\mathbf{r}), \tag{17}$$

where $\bar{a}$ is the effective scattering length, $\rho(\mathbf{r})$ is the deuteron density distribution, μ is the reduced mass of K^--d atoms, M is the nucleon mass, M_A is the target mass, and ω is the Klein-Gordon energy. We choose two sets of the parameterization of $\bar{a}$: One is $\bar{a}=0.34+i0.84$ fm, which is extracted from the fitting to the heavier ($Z\geqslant 3$) kaonic atom data by Batty [23]. This parametrization gives $(\delta E_{1s})_{\rm strong}=-550$ eV (repulsive), $\Gamma_{1s}^{\rm abs}=$ 981 eV, and $\Gamma_{2p}^{\rm abs}=$ 25 meV. The other is $\bar{a}=-0.175+i0.663$ fm, which is obtained from Martin's K-matrix scattering length [8] including the Fermi average and the binding effect. This gives $(\delta E_{1s})_{\rm strong}=-456$ eV, $\Gamma_{1s}^{\rm abs}=$ 652 eV, and $\Gamma_{2p}^{\rm abs}=$ 17 meV. $(\delta E_{1s})_{\rm VP}+(\delta E_{1s})_{\rm FS}$ is 24 eV.

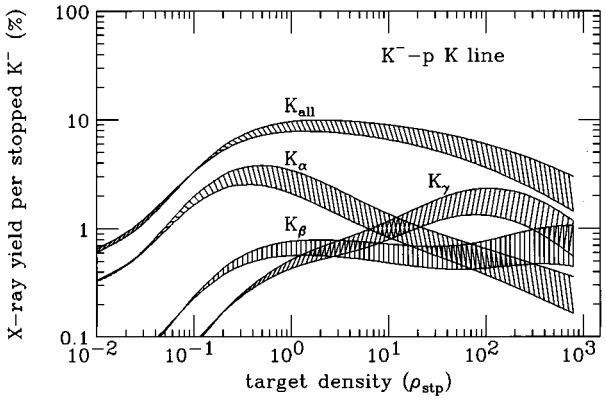

FIG. 7. Density dependence of K^--p atom x-ray yields with varying the free parameter $k_{\rm stk}$ = 1.5–2.5. The shift and width are taken to be $|\delta E_{1s}|_{\rm eff}$ = 300 eV, $\Gamma_{1s}^{\rm abs}$ = 550 eV and $\Gamma_{2p}^{\rm abs}$ = 1 meV.

Figure 10 shows the density dependence of x-ray yields for the two parametrizations and Fig. 11 shows the uncertainty corresponding to $k_{\rm stk}$=1.5–2.5 for the case of Batty's parametrization. The density dependence is similar to the K^--p atom case, except that the x-ray yield is smaller than that of K^--p atoms due to the larger absorption width. Again, the inversion of K_β/K_α and K_γ/K_α ratios appears at a liquid target even when theoretical errors are considered.

The significance of K^--d atom measurements is not limited to the point that the K^--neutron interaction and/or isospin dependence of the K^--N interaction can be extracted. The K^--d atom is concerned with the puzzles for K^--^{4}He atoms: First, it is known that the measured shift and width for K^--^{4}He are larger by one order than those obtained by optical model calculations [14]. Therefore, it should be made clear whether the same situation with K^--^{4}He occurs in the case of K^--d.

The two-body absorption rate of K^- in a nucleus brings another problem. Theoretical two-body absorption rates in light nuclei disagreed with the experimental one [24]. The measurement of K^--d atoms is worth being done from the point of view that K^--d is the most fundamental system concerning the two-body absorption of K^- in a nucleus. For this problem, an estimation of the p-orbit absorption fraction of K^--d atom is needed. However, it is pointed out that the standard Borie-Leon model considerably overestimates the p-orbit absorption fraction even when the x-ray yield is reproduced [18]. On the other hand, Mainz's Monte Carlo approach succeeded in reproducing both of the $\bar{p}$-p atom x-ray data and its p-orbit absorption fraction [16]. Further investigation is required to clarify what is incorrect in the Borie-Leon approach.

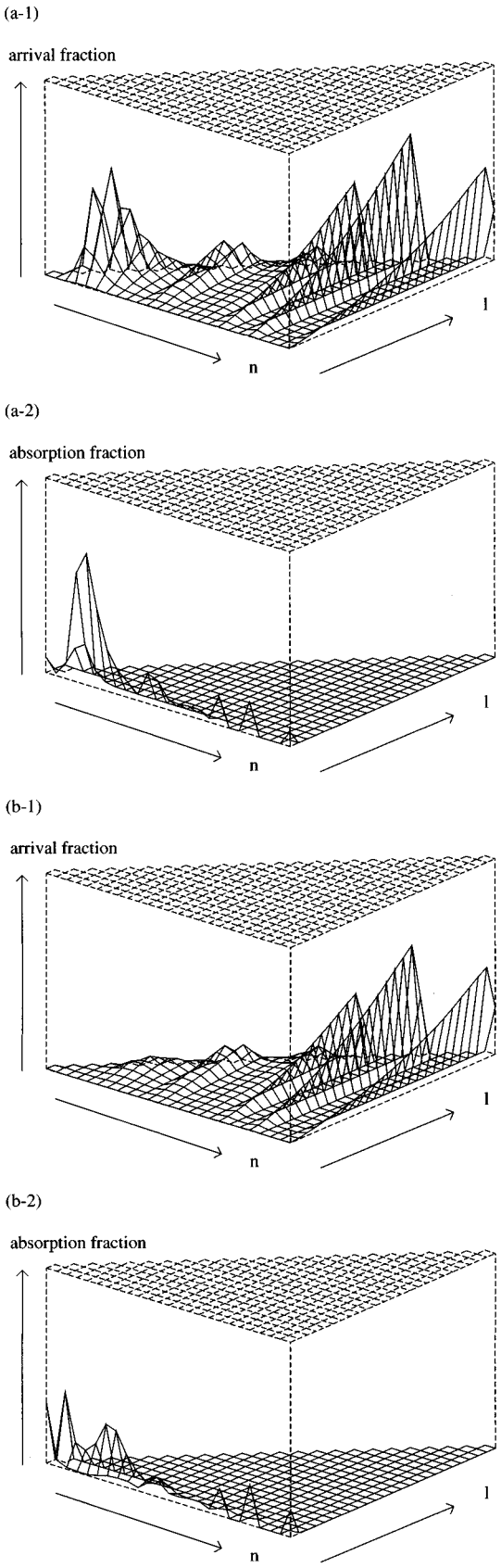

FIG. 8. The stream of cascade-down processes: (a) liquid target, (b) one-atom gas target. The upper figure shows the arrival fraction on each (n, l) level (see the Appendix). The lower figure shows the absorption fraction from each (n, l) level. The scale of the z axis for the arrival fraction is 100 times as large as that for the absorption fraction since the arrival fraction becomes a very large number due to the Stark mixing.

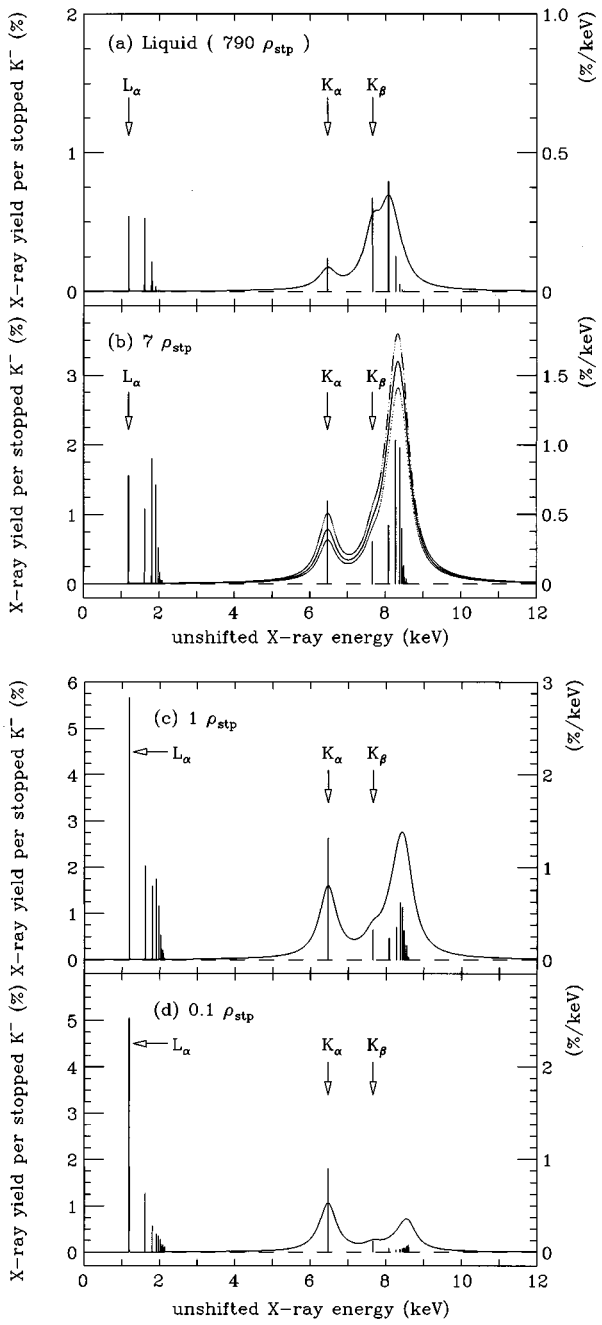

FIG. 9. The expected x-ray spectra: (a) liquid target, (b) seven-atom gas target (KEK experiment [12]), (c) one-atom gas target, and (d) 0.1-atom gas target. The used parameters are $|\delta E_{1s}|_{\rm eff}$ = 300 eV, $\Gamma_{1s}^{\rm abs}$ = 550 eV, $\Gamma_{2p}^{\rm abs}$ = 1 meV, and $k_{\rm stk}$ = 2. The peak shapes are taken to be of Lorentzian form and the detector resolution is not considered. In (b), the cases for $k_{\rm stk}$ = 1.5 (dashed line) and for $k_{\rm stk}$ = 2.5 (dotted line) are also drawn. $k_{\rm stk}$ changes the absolute yields with keeping its spectral shape.

V. CONCLUSIONS

The cascade calculation of K^--p and K^--d atoms is made by using the Borie-Leon model. The parameter concerning the Stark mixing process, $k_{\rm stk}$, is adjusted by fitting antiprotonic and pionic atom data including recently published ones. The density dependence of x-ray yields is investigated with varying the strong-interaction parameters.

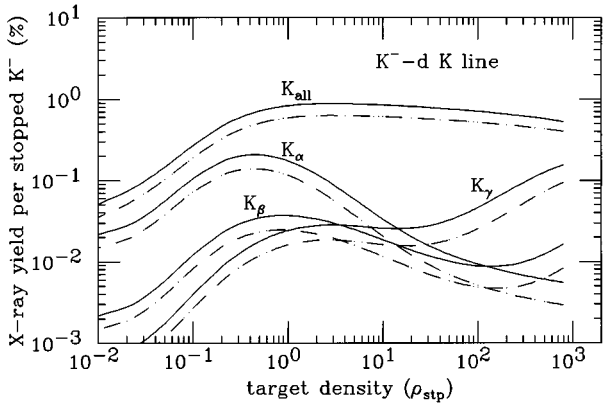

FIG. 10. Density dependence of K^--d atom x-ray yields with varying the strong-interaction parameters. The solid lines are the case of Martin's K matrix + Fermi average + binding effect. The dashed lines are for Batty's optical potential.

The results of K^--p atoms are summarized as follows.

(1) The dependence of x-ray yields on $\Gamma_{1s}^{\rm abs}$ and $(\delta E_{1s})_{\rm strong}$ can be seen only for a high density target, while $\Gamma_{2p}^{\rm abs}$ greatly affects the absolute x-ray yield of K lines at all densities. $\Gamma_{2p}^{\rm abs}>1$ meV is suggested by comparing with the previous x-ray data.

(2) The K_α yield becomes maximum at about one atom gas, though its absolute values are not determined because of the ambiguity of $\Gamma_{2p}^{\rm abs}$. Below one atom, a considerable fraction of K^- decays on atomic orbits by a weak interaction during the cascade-down process. This feature is independent of strong-interaction parameters.

(3) It is expected that the x-ray spectrum shows only two distinct peaks, K_α ($\sim$ 6.5 keV) and the superposition of $K_{\geqslant\beta}$ ($\sim$ 8 keV). The ratio $K_\alpha/K_{\geqslant\beta}$ becomes larger as the target density becomes lower. It is found that the most favorable case for the clear observation of K_α would be about one atom gas target, though the stopping efficiency is low. The ratio $K_\alpha/K_{\geqslant\beta}$ and/or $K_\alpha/L_{\rm all}$ give the information about $\Gamma_{2p}^{\rm abs}$.

In the case of K^--d atom, the x-ray yield is smaller by one order than that of K^--p atoms due to a larger absorption width. Nevertheless, the x-ray measurement is worth being done since it gives information about the isospin dependence of the K^-N interaction, the relation with the puzzle for K^--^{4}He atoms, and the two-body absorption mechanism of the K^- in the nucleus.

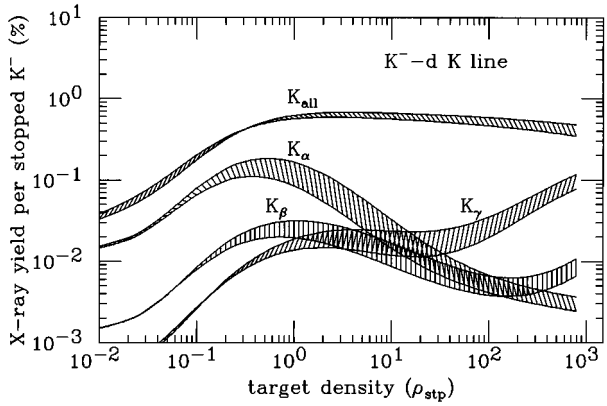

FIG. 11. Density dependence of K^--d atom x-ray yields with varying the free parameter $k_{\rm stk}$ = 1.5–2.5. The strong-interaction parameters are Batty's ones.

ACKNOWLEDGMENTS

The authors would like to thank Dr. M. Iwasaki, Dr. S. N. Nakamura, and T. Ito for information about the KEK PS-E228 experiment. They are also grateful to Prof. R. Seki for valuable comments and discussions about the original code written by E. Borie and M. Leon. Their thanks are also due to Prof. K. Katō and Prof. A. Ohnishi for useful discussions. One of the authors (T.K.) is much indebted to JSPS.

APPENDIX:

In the cascade calculation with Stark mixing, the transition among the same n but different l states causes a difficulty compared with usual cascade calculations. One method is that the reshuffling of the population of the angular momentum states is repeated at each n until the population becomes below a sufficiently small value, for example, 10^{-3}. This procedure is used in Refs. [16,18].

We employ another method using a matrix introduced in Ref. [13]. Let us define $N_{n,l}$ and $\tilde{N}_{n,l}$, where $N_{n,l}$ is the starting population of the (n,l) level before Stark mixing and $\tilde{N}_{n,l}$ is the arrival fraction of (n,l) level resulting from Stark mixing. Then, the relation

$$\tilde{N}_{n,l}=N_{n,l}+\tilde{N}_{n,l+1}\frac{\Gamma^{\rm Stark}_{n,l+1\to {\rm n},l}}{\Gamma^{\rm total}_{n,l+1}}+\tilde{N}_{n,l-1}\frac{\Gamma^{\rm Stark}_{n,l-1\to {\rm n},l}}{\Gamma^{\rm total}_{n,l-1}}, \tag{A1}$$

$$\Gamma^{\rm total}_{n,l}=\sum_{n'<n,l'}(\Gamma^{\rm mol}_{n,l\to n',l'}+\Gamma^{\rm Aug}_{n,l\to n',l'}+\Gamma^{\rm rad}_{n,l\to n',l'}) +\Gamma^{\rm abs}_{n,l}+\Gamma^{\rm weak}+\Gamma^{\rm Stark}_{n,l\to n,l+1}+\Gamma^{\rm Stark}_{n,l\to n,l-1} \tag{A2}$$

holds for each (n,l) level. Now, the n-dimensional vectors $\boldsymbol{N}_n$, $\tilde{\boldsymbol{N}}_n$ are introduced by

$$\boldsymbol{N}_n=\begin{pmatrix} N_{n,l=0} \\ \vdots \\ N_{n,l=n-1}\end{pmatrix},\quad \tilde{\boldsymbol{N}}_n=\begin{pmatrix} \tilde{N}_{n,l=0} \\ \vdots \\ \tilde{N}_{n,l=n-1}\end{pmatrix}. \tag{A3}$$

Then, Eq. (18) for $l=0\sim n-1$ becomes

$$A\tilde{\boldsymbol{N}}_n=\boldsymbol{N}_n, \tag{A4}$$

where A is the following $n\times n$ matrix:

$$A=\begin{pmatrix} 1 & -\frac{\Gamma^{\rm Stark}_{n,\,1\rightarrow\,n,\,0}}{\Gamma^{\rm total}_{n,\,1}} & 0 & \cdots & 0 & 0 \\ -\frac{\Gamma^{\rm Stark}_{n,\,0\rightarrow\,n,\,1}}{\Gamma^{\rm total}_{n,\,0}} & 1 & -\frac{\Gamma^{\rm Stark}_{n,\,2\rightarrow\,n,\,1}}{\Gamma^{\rm total}_{n,\,2}} & \cdots & 0 & 0 \\ 0 & -\frac{\Gamma^{\rm Stark}_{n,\,1\rightarrow\,n,\,2}}{\Gamma^{\rm total}_{n,\,1}} & 1 & \cdots & 0 & 0 \\ \vdots & \vdots & \vdots & \ddots & \vdots & \vdots \\ 0 & 0 & 0 & \cdots & 1 & -\frac{\Gamma^{\rm Stark}_{n,n-\,1\rightarrow\,n,n-2}}{\Gamma^{\rm total}_{n,n-\,1}} \\ 0 & 0 & 0 & \cdots & -\frac{\Gamma^{\rm Stark}_{n,n-\,2\rightarrow\,n,n-1}}{\Gamma^{\rm total}_{n,n-\,2}} & 1 \end{pmatrix}, \tag{A5}$$

and the solution is given by

$$\tilde{\boldsymbol{N}}_n = A^{-1}\boldsymbol{N}_n\,. \tag{A6}$$

The deexciting, absorbing, and weak-decaying fractions at each (n,l) level are

$$f^{\rm deexcite}_{n,l\rightarrow n',l'}=\tilde{N}_{n,l}\frac{\Gamma^{\rm mol}_{n,l\rightarrow n',l'}+\Gamma^{\rm Aug}_{n,l\rightarrow n',l'}+\Gamma^{\rm rad}_{n,l\rightarrow n',l'}}{\Gamma^{\rm total}_{n,l}}, \tag{A7}$$

$$f^{\rm abs}_{n,l}=\tilde{N}_{n,l}\frac{\Gamma^{\rm abs}_{n,l}}{\Gamma^{\rm total}_{n,l}}, \tag{A8}$$

$$f^{\rm weak}_{n,l}=\tilde{N}_{n,l}\frac{\Gamma^{\rm weak}}{\Gamma^{\rm total}_{n,l}}. \tag{A9}$$

This procedure is repeated from $n=n_{\rm max}$ to $n=1$.

[1] For example, M. Arima and K. Yazaki, Nucl. Phys. **A506**, 553 (1990).
[2] J. D. Davies, G. J. Pyle, G. T. A. Squier, C. J. Batty, S. F. Biagi, S. D. Hoath, P. Sharman, and A. S. Clough, Phys. Lett. **83B**, 55 (1979).
[3] M. Izycki, G. Backenstoss, L. Tauscher, P. Blüm, R. Guigas, N. Hassler, H. Kock, H. Poth, K. Fransson, A. Nilsson, P. Pavlopoulos, and K. Zioutas, Z. Phys. A **239**, 11 (1980).
[4] P. M. Bird, A. S. Clough, K. R. Parker, G. J. Pyle, G. T. A. Squier, S. Baird, C. J. Batty, A. I. Kilvington, F. M. Russell, and P. Sharman, Nucl. Phys. **A404**, 482 (1983).
[5] J. K. Kim, Ph.D. thesis, Columbia University, 1966.
[6] Y. A. Chao, R. W. Kraemer, D. W. Thomas, and B. R. Martin, Nucl. Phys. **B56**, 46 (1973).
[7] A. D. Martin and G. G. Ross, Nucl. Phys. **B16**, 479 (1970).
[8] A. D. Martin, Nucl. Phys. **B179**, 33 (1981).
[9] R. H. Dalitz, J. McGinley, C. Beyea, and S. Anthony, in Proceedings of the International Conference on Hypernuclear and Kaon Physics, Heidelberg, Germany 1982, Report No. MPIH-1982-V20.
[10] J. E. Conboy, D. J. Miller, N. Bedford, D. Evans, T. Fallahi, J. V. Major, and T. Tymieniecka, J. Phys. G **12**, 1143 (1986).
[11] K. Tanaka and A. Suzuki, Phys. Rev. C **45**, 2068 (1992).
[12] M. Iwasaki *et al.*, KEK PS-E228 experiment.
[13] E. Borie and M. Leon, Phys. Rev. A **21**, 1460 (1980).
[14] C. J. Batty, Nucl. Phys. **A508**, 89c (1990).
[15] G. Reifenröther and E. Klempt, Phys. Lett. B **248**, 250 (1990).
[16] G. Reifenröther and E. Klempt, Nucl. Phys. **A503**, 885 (1989).
[17] M. Leon and H. A. Bethe, Phys. Rev. **27**, 636 (1962).
[18] C. J. Batty, Rep. Prog. Phys. **52**, 1165 (1989).
[19] K. Heitlinger, R. Bacher, A. Badertscher, P. Blüm, J. Eades, J. Egger, K. Elsener, D. Gotta, E. Morenzoni, and L. M. Simons, Z. Phys. A **342**, 359 (1992).
[20] A. J. Rusi El Hassani *et al.*, Z. Phys. A **351**, 113 (1995).
[21] J. F. Crawford, M. Daum, R. Frosch, B. Jost, P.-R. Kettle, R. M. Marshall, B. K. Wright, and K. O. H. Ziock, Phys. Rev. D **43**, 46 (1991).
[22] S. Deser, M. L. Goldberger, K. Baumann, and W. Thirring, Phys. Rev. **96**, 774 (1954).
[23] C. J. Batty, Nucl. Phys. **A372**, 418 (1981).
[24] T. Onaga, H. Narumi, and T. Kohmura, Prog. Theor. Phys. **82**, 222 (1989).
[25] W. Beer *et al.*, Phys. Lett. B **261**, 16 (1991).
[26] D. Chatellard *et al.*, Phys. Rev. Lett. **74**, 4157 (1995).